Experimental and theoretical study of ozone adsorption on alumina

K. Thomas, P.E. Hoggan, L. Mariey, J. Lamotte and J.C. Lavalley

Laboratoire Catalyse et Spectrochimie UMR CNRS 6506 – ISMRA, 6 Boulevard du Maréchal Juin, 14050 Caen Cedex, France

Received 5 February 1997; accepted 26 March 1997

Ozone adsorption has been studied by IR spectroscopy at low temperature. Although alumina is more acidic than TiO_2, as shown by pyridine adsorption, IR spectroscopy did not detect O_3 species adsorbed on strong Lewis Al^{3+} sites. However, O_3 decomposition occurred and pyridine specific poisoning evidenced that such sites were involved in the decomposition. Quantum chemistry calculations confirmed such a result and specified that the remaining $O(^1D)$ resulting from the decomposition, in addition to physisorbed O_2, was attached to the aluminum ion constituting the Lewis sites. The oxygen molecules would then gradually be desorbed.

Keywords: ozone, alumina, infrared spectroscopy, quantum chemistry, embedded-cluster, reaction pathway

1. Introduction

Catalytic ozone decomposition is of practical importance to eliminate toxic ozone. In a previous paper [1] we showed by infrared spectroscopy at liquid nitrogen temperature that ozone adsorption on titania occurred on Lewis acid sites. When their strength is sufficiently great, they are able to provoke ozone dissociation even at such a low temperature.

The aim of the present paper is to extend the work to alumina, which is also able to dissociate ozone [2]. Since no direct information can be obtained from infrared studies, ozone dissociation has been followed by pressure measurements in the cell. Specific poisoning experiments with pyridine have been carried out to determine the nature of the dissociative adsorption sites on alumina. The work is complemented by quantum chemistry calculations which specify the ozone dissociation mechanism.

2. Experimental

2.1. Infrared study

The stainless steel cell for studying the infrared spectra of adsorbed species at 77 K was described previously [3]. γ-alumina (Rhône-Poulenc GCO, specific area 250 $m^2\ g^{-1}$) was pressed into pellets (10–20 mg), and pretreated in a vacuum at 770 K for 4 h.

For experiments performed on alumina pretreated by pyridine, 1 Torr of pyridine was introduced at room temperature, then evacuated at 320 K or at 420 K. Weakly dehydroxylated alumina was obtained introducing 3 Torr of water at room temperature, then evacuating at 470 K.

Ozone was prepared from gaseous O_2 in an electric discharge at room temperature and introduced into the cell at 77 K. All spectra were recorded on a 710 Nicolet FT-IR spectrometer at 77 K. Reported spectra were subtracted from those of the cooled, pretreated samples. The pressure in the cell was followed with time using a Barocel 600 gauge (Datametrics).

2.2. Quantum chemistry calculations

First, careful ab initio calculations over Slater type atomic orbital bases were carried out using the STOP [4] package for the isolated ozone molecule. The results were interpreted using localised partial charge calculations [5] in order to investigate the polarity of the three oxygen atoms.

Previous results involving molecular adsorption on metal oxide surfaces have shown that embedded cluster techniques correctly account for both local and long-range interactions involved in adsorbate–substrate systems [6]. The alumina surface required a site containing too many atomic orbitals to be treated at the ab initio level using STOP without prohibitively long calculation times. However, the embedding technique is available in the GEOMOS [7] semi-empirical package which also uses Green's matrix approach to evaluate the molecular orbitals of the adsorbate-site supermolecule under the influence of the bulk solid perturbation potential.

We therefore used GEOMOS throughout the present study. Out of a wide choice of semi-empirical hamiltonians, MNDO2 [8] was chosen for the present study, because it also uses a Slater type atomic orbital basis and can be extended to metal atoms including transition metals. It is therefore well suited to interaction studies. All the structures studied were optimised using the Rinaldi conjugate gradient method in GEOMOS based on the BFGS [9] algorithm.

The fact that the product of ozone decomposition

involves a doublet spin-state required that all the SCF calculations be performed for open-shells at the unrestricted Hartree–Fock level (UHF).

Once the local SCF for physisorbed ozone had been established, the terminal O–O linkage was frozen then increased step by step in order to simulate advance along the reaction co-ordinate for ozone decomposition. The geometry was optimised at each step and the local SCF calculation then carried out and embedded in the γ-Al_2O_3 bulk potential (initially periodic).

All the quantum chemistry calculations were carried out on an IBM RS 6000-3BT workstation running at 50 MIPS. The software used was STOP and GEOMOS (in-house versions of GCPE 667 and 584 respectively) using ESSL library routines for the linear algebra and quadratures. CERIUS2 molecular simulations program [10] was used for visualisation, to facilitate data input while constructing the substrate active site and to provide graphics.

3. Results

3.1. Infrared study

Let us recall that O_3 adsorption on silica leads to hydrogen-bonded species characterized by O_3 bands near 1104 (ν_1) and 1037 cm^{-1} (ν_3). Due to silica absorption of the IR beam in this frequency range, those wavenumbers have been calculated, using $\nu_1 + \nu_3$ combination band, $2\nu_3$ overtone, and $^{18}O_3$ adsorption results [11]. In the case of titania another type of species is detected and characterized by bands at 1144 (ν_1) and 994 cm^{-1} (ν_3). Previous experiments showed that such bands are due to coordination of O_3 on strong Lewis acid sites. Such an adsorption activates the O_3 molecule which decomposes into an oxygen molecule and atomic oxygen [1].

It is well known that alumina presents stronger Lewis sites than TiO_2. For instance, figure 1 shows the

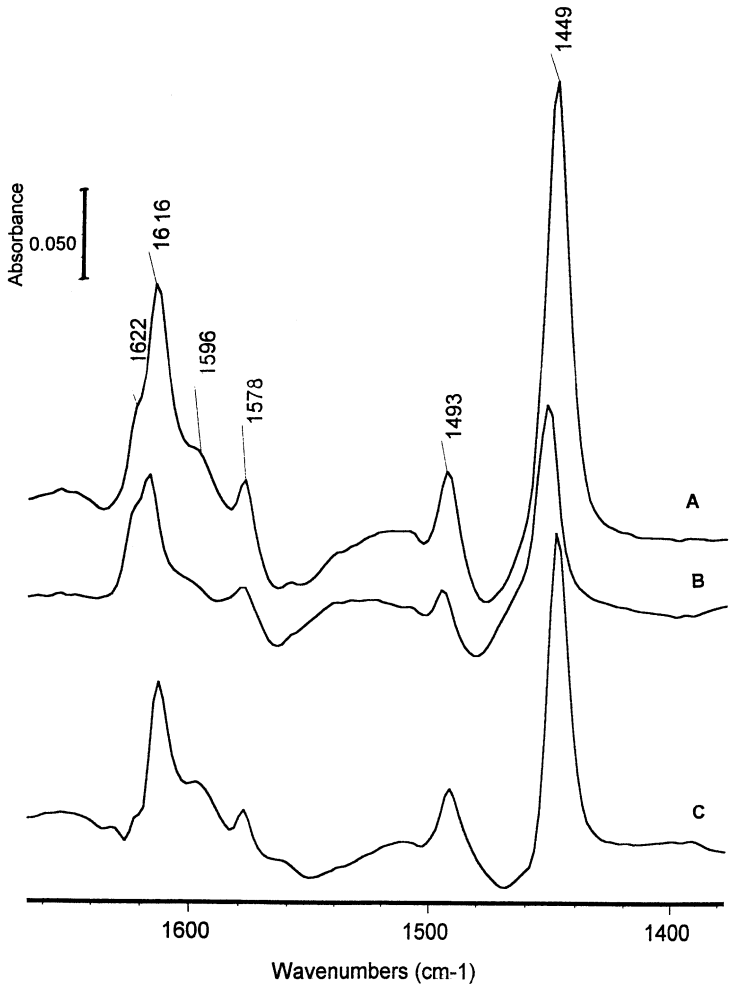

Figure 1. Spectrum of pyridine adsorbed at room temperature on alumina, then evacuated (A) at 320 K, (B) at 420 K, (C) difference A minus B.

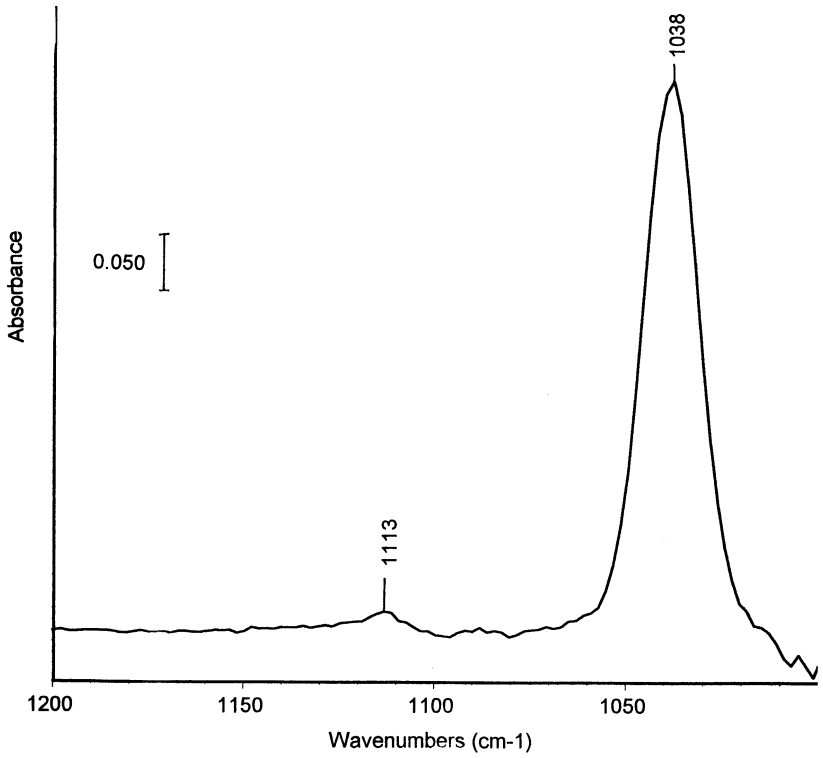

Figure 2. Spectrum of ozone adsorbed at 77 K on alumina.

IR bands of pyridine species on Al_2O_3. The band at 1616 cm^{-1} (ν_{8a}) with a shoulder near 1622 cm^{-1} characterizes pyridine (py) adsorption on strong Lewis sites. On titania, this mode is observed at 1612 cm^{-1} revealing weaker acidity [12]. Subtraction spectra evidence that, in addition to weakly adsorbed py species characterized by bands near 1596 and 1578 cm^{-1}, about half of the coordinatively unsaturated aluminum sites, giving rise to the 1616 cm^{-1} band after py adsorption, have been liberated by evacuation temperature increase from 320 to 420 K.

O_3 adsorption on alumina (figure 2) leads to a weak band at 1113 cm^{-1} (ν_1) and a stronger band at 1038 cm^{-1} (ν_3). Their wavenumbers are very close to those observed for physisorbed or weakly adsorbed species, which is

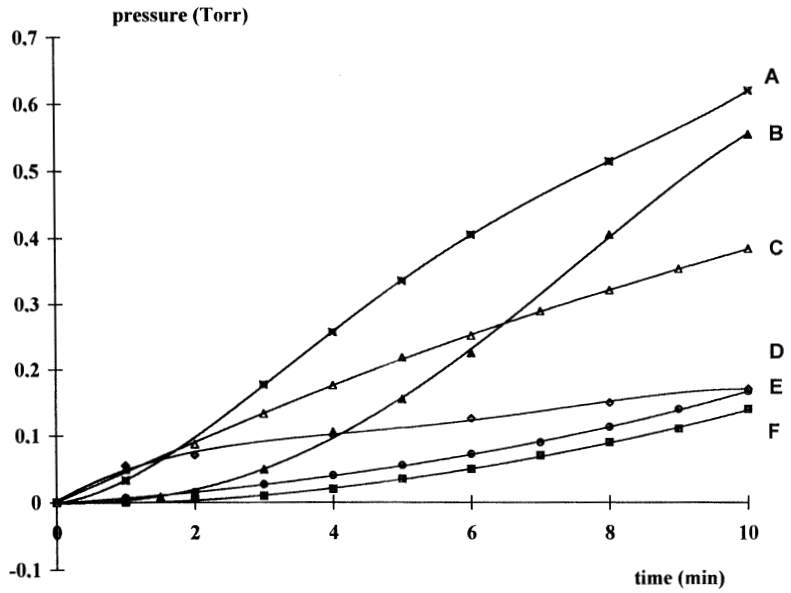

Figure 3. Evolution of O_2 pressure in the IR cell for various samples. (A) Al_2O_3, (B) Al_2O_3 + pyridine evacuated at 420 K, (C) TiO_2, (D) SiO_2, (E) Al_2O_3 weakly dehydroxylated, (F) Al_2O_3 + pyridine evacuated at 320 K.

confirmed by the very low intensity ratio I_{ν_1}/I_{ν_3}. In particular no bands near 1150 and 990 cm^{-1}, expected for O_3 coordinated on strong Lewis sites are observed. Note the same O_3 bands are observed on the pyridine precovered samples.

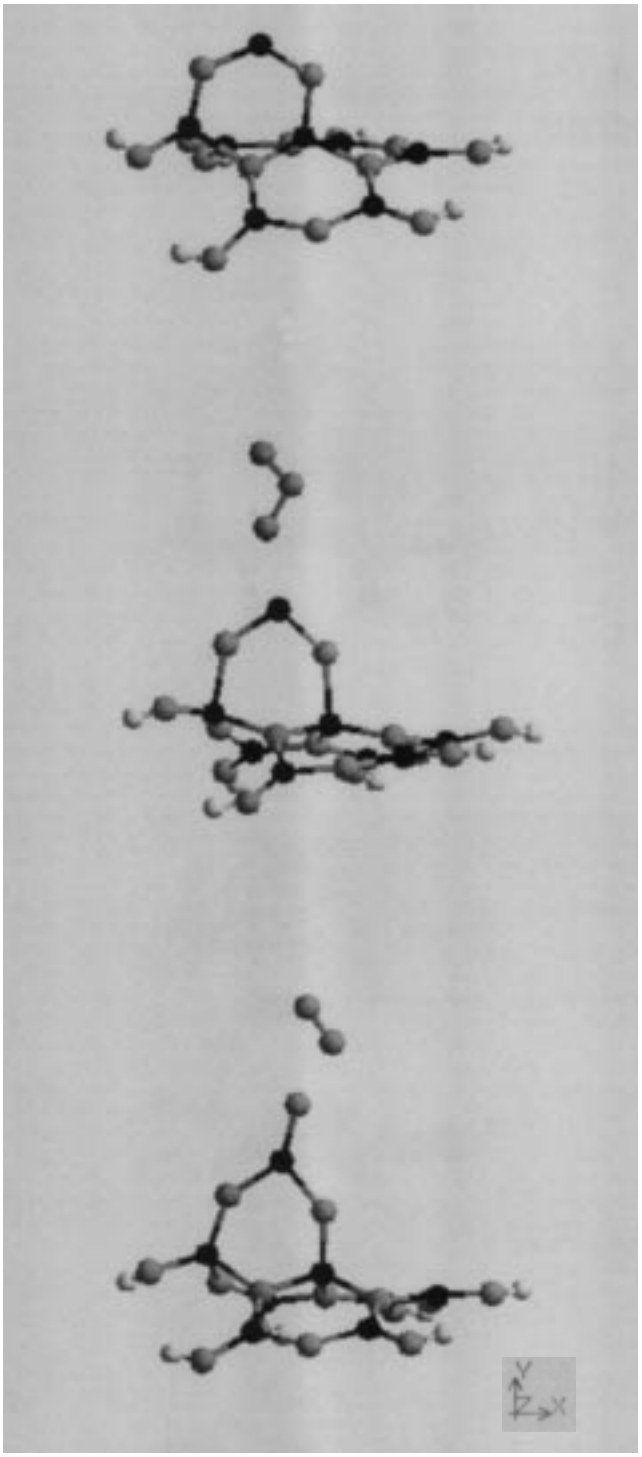

Figure 4. Alumina supermolecule representing active sites. Black atoms are aluminum atoms. Grey atoms are oxygen atoms. White atoms are hydrogen atoms.

To determine whether O_3 dissociation occurs even at 77 K, we have followed the pressure in the cell at this temperature as a function of time (figure 3). A very slight pressure increase is observed on silica. It is more pronounced on TiO_2 and even more on activated alumina. It clearly appears that the stronger the Lewis acidity, the faster the O_3 decomposition is. It is remarkable that on the alumina sample which is fully covered with pyridine, almost no O_3 decomposition occurs, not even on a fully hydroxylated alumina sample. By contrast, pyridine evacuation at 420 K has regenerated a portion of the strong Lewis acid sites, allowing a partial recovery of the O_3 decomposition activity. In no case does O_3 react with pyridine.

These experiments indicate that the alumina Lewis acid centres are the active sites for O_3 decomposition. Their strength is sufficiently high to prevent any observation of O_3 adsorption on them, since it is transitory under the present conditions, which confirms previous results obtained on highly activated titania [1].

3.2. Quantum chemistry calculations

The adsorbate active site was gradually built up from Al_2O_3 units and found to form a hexagonal structure at the energy minimum.

Once size-consistency had been reached, the site with a bridging O–Al–O unit to represent the Lewis acid center (figure 4) was optimised in the presence of an ozone molecule.

The ozone molecule which was initialised using the geometry obtained with the STOP package was found to settle at a local minimum corresponding to a polarisation interaction. This defines the starting point of the reaction coordinate (scheme 1).

This confirmed that the terminal O_3 atoms have a net negative charge whereas the central atom has the compensating net positive charge. The absolute values of these charges for the closed-shell ground state of the ozone molecule compare favorably with quantum chemical studies using various reliable methods by other authors [13], using a double-zeta STO basis which has been optimised for oxygen atoms.

Two initial positions for the ozone molecule were chosen: the first with $d = 1.3$ Å and the second with $d = 2$ Å, where d is the distance between the terminal oxygen of ozone and the Lewis center (aluminum) of the alumina surface. These two choices of initial d are based on placing the molecule in the repulsive and attractive region of the interaction potential, respectively. Table 1 contains salient geometric parameters (bond lengths and valence angles) for ozone adsorption on alumina.

The other interatomic distances plotted are those between the aforementioned aluminum (1) and the oxygen atoms of ozone (2, 3, 4). The ozone valence angle is included. Their values clearly show that the

species present after optimisation is dioxygen (O_2) and that the remaining oxygen atom is linked to the aluminum. The decomposition therefore proceeds very readily.

Both initial positions lead to local energy minima far more stable than the reactants. That resulting from the initial $d = 1.3$ Å has O_2–O 2.1 Å apart and corresponds to a physisorbed O_2 molecule. The ozone decomposition is strongly exothermic and a slightly lower minimum is obtained when $d = 2$ Å initially with a large O_2–O separation (8.5 Å) consistent with our finding that the separate products correspond to lowest energy.

We would expect to find some physisorbed oxygen whereas desorption of gaseous oxygen will dominate more as the temperature increases. This nicely corroborates the experimentally measured increase in oxygen pressure observed in the IR reactant cell, after ozone adsorption on alumina.

The energy profile for ozone decomposition is represented in figure 5.

The steep portion of the energy profile curve for reaction coordinate values around 1.7–1.8 Å corresponds to the sharp energy stabilisation accompanying rapid decomposition of the ozone molecule when the O(2)–O(3) linkage is broken.

During the subsequent desorption of the ozone molecule, we initially observed a shallow well corresponding to physisorbed dioxygen at around 2 Å. A fairly low desorption barrier is located around 2.34 Å about 3 kcal mol^{-1} in height. This is readily accessible even at low temperature.

The supermolecule representing the active site on the alumina surface is illustrated in figure 4a. The initial position of the ozone molecule is obtained by placing it close to the site in its ab initio geometry (figure 4b). The whole adsorbate–substrate system is then embedded in the bulk alumina potential and the result of optimisation (figure 4c) clearly shows the physisorbed dioxygen molecule.

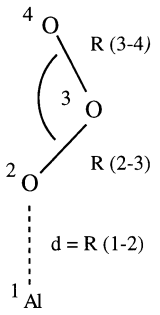

Scheme 1. Definition of reaction coordinate.

4. Conclusion

The present paper provides ample evidence from both FTIR measurements and quantum chemistry calculations that ozone decomposition occurs readily on the alumina surface.

These results are in perfect agreement and indicate that the reaction occurs even at liquid nitrogen temperature. The products are shown to be molecular oxygen (in the ground-state triplet) and a nascent oxygen atom (singlet D state) incorporated into the surface. These products in the reaction pathway calculation correspond perfectly to the rise in oxygen pressure observed in the reactor cell.

The fact that strong Lewis acid sites (aluminum ions) are responsible for this catalytic ozone decomposition is confirmed by the calculations and also by an experiment in which these sites were selectively poisoned with pyridine. This led to almost no oxygen in the product.

Table 1
Geometric and charge parameters for O_3 adsorption on alumina according to the d distances (distance in Å, angles and net atomic charges)

	$d = 1.3$		$d = 2$	
	before optimisation	after optimisation	before optimisation	after optimisation
geometric values				
$R(1-2)$	1.3	1.735	2	1.725
$R(2-3)$	1.223	*2.071*	1.223	*8.530*
$R(3-4)$	1.223	1.171	1.223	1.169
angle 234	114°57	154°58	114°57	249°47
net atomic charge				
1 (Al)	+0.023	+0.857	+0.023	
2 (O)	−0.3	−0.3270	−0.3	−0.324
3 (O)	+0.6 (O_3)	+0.063 (O_2)	+0.6 (O_3)	+0.0017 (O_2)
4 (O)	−0.3	−0.063	−0.3	−0.0621
reaction energy (kcal/mol)		−134.62		−140.35

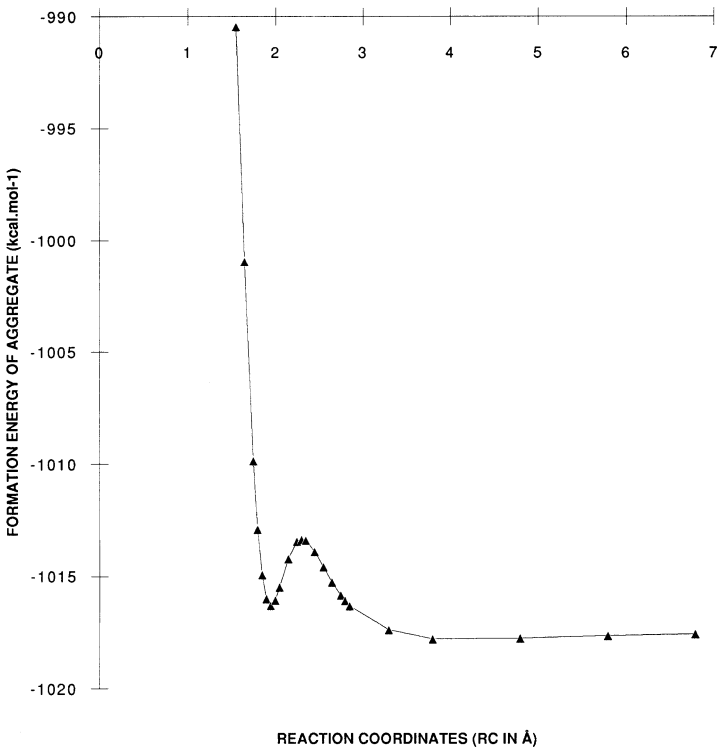

Figure 5. Energy profile for ozone decomposition / oxygen desorption.

This combined study confirms and extends the information which could be deduced by analogy with previous work on titania and provides a mechanistic insight into catalytic ozone decomposition.

References

[1] K.M. Bulanin, A.V. Alexeev, D.S. Bystrov, J.C. Lavalley and A.A. Tsyganenko, J. Phys. Chem. 99 (1995) 10294.
[2] A.O. Klimovski, A.V. Bavin, V.S. Tkalich and A.A. Lisachenko, React. Kinet. Catal. Lett. 23 (1983) 95.
[3] M.A. Babaeva, D.S. Bystrov, A.Y. Kovalgin and A.A. Tsyganenko, J. Catal. 123 (1990) 396.
[4] STOP: Slater Type Orbital Package, A. Bouferguene and P.E. Hoggan, QCPE 667 (1996).
[5] F. Audry, P.E. Hoggan, J. Saussey, J.C. Lavalley, H. Lauron-Pernot and A.M. Le Govic, J. Catal., accepted.
[6] P.E. Hoggan, M. Bensitel and J.C. Lavalley, J. Mol. Struct. 44 (1994) 320.
[7] GEOMOS: Geometry Optimisation of Molecule Orbitals with Solid Solvent effects, D. Rinaldi, P.E. Hoggan and A. Cartier, QCPE 584 (1989).
[8] P.E. Hoggan and D. Rinaldi, Theor. Chim. Acta. 72 (1987) 467.
[9] G. Broydon, R. Fletcher, M.G. Goldfarb and C. Shanno, Comp. J. 13 (1970) 185.
[10] CERIUS2 molecular simulations (1995).
[11] K.M. Bulanin, A.V. Alexeev, D.S. Bystrov, J.C. Lavalley and A.A. Tsyganenko, J. Phys. Chem. 98 (1994) 5100.
[12] C. Morterra, G. Ghiotti and E. Garrone, J. Chem. Soc. Faraday I 76 (1980) 2102.
[13] R.G. Jones, J. Chem. Phys. 82 (1985) 111.